

# Cu K-edge Resonant Inelastic X-Ray Scattering in Edge-Sharing Cuprates

F. Vemay<sup>1,2</sup>, B. Moritz<sup>1,2</sup>, T. P. Devereaux<sup>1,2</sup>, and G. A. Sawatzky<sup>2,3</sup>

<sup>1</sup>University of Waterloo, Waterloo, Ontario N2L 3G1, Canada

<sup>2</sup>Pacific Institute of Theoretical Physics, University of British Columbia, Vancouver BC and

<sup>3</sup>Department of Physics, University of British Columbia, Vancouver, BC

(Dated: May 26, 2019)

We present calculations for resonant inelastic x-ray scattering (RIXS) in edge-shared copper oxide systems, such as  $\text{CuGeO}_3$  and  $\text{Li}_2\text{CuO}_2$ , appropriate for hard x-ray scattering where the photoexcited electron lies above oxygen 2p and copper 3d orbital energies. We perform exact diagonalizations of the multi-band Hubbard and determine the energies, orbital character and resonance profiles of excitations which can be probed via RIXS. We find excellent agreement with recent results on  $\text{Li}_2\text{CuO}_2$  and  $\text{CuGeO}_3$  in the 2-7 eV photon energy loss range.

PACS numbers:

Techniques that probe the momentum dependence of strongly correlated electrons provide valuable information that can be used as a test for models appropriate for the cuprates. angle-resolved photoemission (ARPES) provides important information about single-particle excitations of occupied states [3], and recently has been extended to several electron volts below the Fermi surface [2]. Electronic Raman scattering reveals information about multiparticle excitations at long wavelengths [4]. Resonant inelastic x-ray scattering (RIXS) recently has undergone vast improvements, allowing probes of momentum dependent excitations into unoccupied states [5]. Improvements in resolution now offer the possibility of a direct comparison of ARPES, Raman, and RIXS spectra in the several eV range with the hope of understanding the nature of strong correlations in the cuprates, and high temperature superconductivity, by studying electronic excitations at several energy scales.

As a fundamental building block of low-energy effective theories of the cuprates, the Zhang-Rice singlet (ZRS) [1] is the starting point of the single-band Hubbard and t-J models widely believed to capture the low energy physics of strongly correlated systems. It is well-known that the ZRS features prominently in RIXS in the cuprates. A particular test of models of the cuprates lies in the difference between RIXS in edge-shared versus corner-shared copper oxide systems. In materials such as  $\text{La}_2\text{CuO}_4$  and other corner sharing 2D members of the high  $T_c$  family, the ZRS is stabilized by a strong gain in antiferromagnetic exchange energy between Cu and O, and can propagate to neighboring  $\text{CuO}_4$  plaquettes, with effective hopping  $t = 0.35$  eV along the Cu-O bond direction, and  $t^0 = 0.15$  eV along the diagonal [1]. In edge-shared cuprates, such as  $\text{CuGeO}_3$  and  $\text{Li}_2\text{CuO}_2$ , the Cu-O-Cu bond approximately forms a 90-degree angle [6], compared to 180 in corner-shared cuprates, and therefore according to Goodenough-Kanamori-Anderson [7], the nearest-neighbor copper-copper exchange tends to be slightly ferromagnetic. However, higher order processes like Cu-O-Cu hopping also contribute comparable antiferromag-

netic exchange terms. For these reasons, small bond-angle variations among different edge-sharing compounds can make the exchange slightly anti-ferromagnetic or ferromagnetic. In either case, the ZRS is less stable and mobile due to hybridization among different oxygen orbitals not aligned with  $\text{Cu } d_{x^2-y^2}$  orbitals [6].

Recent Cu K-edge RIXS data on edge-sharing cuprate  $\text{Li}_2\text{CuO}_2$  [8, 9] has revealed a small, non-dispersive peak at 2.1 eV, attributed to interatomic d-d excitations, a strong peak at 5.4 eV, and a weak peak at 7.6 eV, both attributed to charge transfer excitations. The peak at 5.4 eV is doubly resonant for incident photon energies near 8986 and 9000 eV [8]. In  $\text{CuGeO}_3$ , clear excitations were found are 3.8 eV (weak) and 6 eV (strong) [9, 10, 11], and more recently 1.7 eV [12], which were attributed in Ref. [12] as an intra-atomic d-d excitation (1.7 eV), a ZRS excitation (3.8 eV), and a charge transfer excitation on a single copper oxide plaquette (6.4 eV). Similar features have also appeared in oxygen 1s RIXS [13]. While a few momentum-dependent studies have been performed, the incident photon energy dependence, or resonance profile, is usually shown only for a few selected points in the Brillouin zone.

In this paper we present exact diagonalizations of Hubbard clusters of edge-sharing copper oxide plaquettes shown in Fig. 1. We calculate both the RIXS spectrum and the resonance profile for several cluster geometries, and determine the nature of excitations accessible via light scattering. We pay special attention to the intermediate core-hole and  $n$ -excited-state wavefunctions of RIXS accessible states. We find good agreement with the results on edge-shared copper oxide systems, and confirm excitation assignments of Ref. 12.

The RIXS process consists in sending a photon of energy  $\sim \omega_i$  on a sample in the ground state  $|j_0\rangle$  having energy  $E_0$ . For K-edge RIXS, an electron from the 1s copper-core is photoexcited into the Cu 4p-band, leaving behind a core hole. The strong Coulomb repulsion between the core hole and  $d_{x^2-y^2}$  holes on the same Cu atom reorganizes charge density, forming an intermediate

state  $|j_{ci}\rangle$  of eigenenergy  $E_{ci}$ . The 4p electron recom - bines with the 1s core hole with an energy transfer  $\sim \omega$ ,

leaving the system in the final state  $|j_f\rangle$  of eigenenergy  $E_f$ . The RIXS intensity spectrum is thus given by [5]:

$$I(|j_f\rangle; \omega = E_f - E_i) / \sum_{f,i} \sum_{4p,1s} \frac{|\langle j_f | \hat{h}_{ci} | i \rangle|^2}{E_{ci} + \epsilon_{4p,1s} - E_0 - \gamma} (E_f - E_i - \omega)^2 \quad (1)$$

Here  $\epsilon_{4p,1s}$  represents the Cu 1s - 4p energy separation. For simplicity we neglect specific 4p orientation and photon polarizations. The parameter  $\gamma$  represents damping of the intermediate state due to fluorescence and Auger 1s decay, which we take as 1.0 eV. While this value determines the overall resonant enhancement, it does not affect the resolution of the energy-loss peaks in the spectrum. We broaden the delta function with a width 0.1eV to represent current instrument resolution.

The Hamiltonian describing the open boundary cluster shown in Fig. (1), with rotated  $x$  and  $y$  directions along the p orbitals, is given by  $H = \sum_{ij} H_{ij}^K + \sum_i (H_i^U + H_i^P) + U_Q \sum_i (d_{i0}^V, d_{i0})$ , with

$$\begin{aligned} H_{ij}^K &= t_{pd} P_{i,j}^Y P_{i,j}^Y d_j + t_{pdz} P_{i,j}^Z P_{i,j}^Y d_z + j \\ &+ t_{pp} P_{i,j}^0 P_{i,j}^Y P_j + t_{pp}^0 P_{i,j}^Y P_j + h.c \\ H_i &= \epsilon_i^p (P_i^Y P_i + P_i^0 P_i) + \epsilon_i^d d_{i,z}^Y d_{i,z} + \epsilon_i^d d_{i,z}^Y d_{i,z} \\ H_i^U &= U_{pp} P_{i,1}^Y P_{i,2}^Y P_{i,3}^Y P_{i,4}^Y + U_{pp} P_{i,1}^0 P_{i,2}^0 P_{i,3}^0 P_{i,4}^0 \\ &+ U_{dd} d_{i,1}^Y d_{i,2}^Y d_{i,3}^Y d_{i,4}^Y + U_{dd} d_{i,1}^Y d_{i,2}^Y d_{i,3}^Y d_{i,4}^Y : \end{aligned}$$

Here  $d_{i,z}^Y$ ;  $d_{i,z}^0$ ;  $P_i^Y$ ;  $P_i^0$  and  $d_{i,x}$ ;  $d_{i,z}$ ;  $P_i^Y$ ;  $P_i^0$  creates and annihilates a  $d_{x^2-y^2}$ ,  $d_{3z^2-r^2}$ , planar p or  $p^0$  hole with spin at site  $i$ , respectively, and the sum runs over nearest neighbors. The hopping amplitude  $t_{pp}$  refers to the hopping between two nearest p-p orbitals with  $\epsilon$ , and  $t_{pp}^0$  refers to the hopping between two nearest-neighbor p-oxygen orbitals, where  $\epsilon = x/y$ . The overlap phase factors are chosen such that  $P_{i,j} = 1$  for neighbors in the  $x$ ;  $y$  direction, and  $-1$  for  $x/y$ . The oxygen phase factors are analogously defined as  $P_{i,j}^0 = 1$  for oxygens at  $x/y$  and  $-x/y$ , and  $-1$  for the other combinations. Here  $s_0$  (resp.  $s_0^Y$ ) creates (annihilates) a  $Cu_{1s}$  core-electron. Here  $U_Q$  is the core-d hole repulsion. For simplicity we neglect interactions involving the 4p photo-excited electron, such as the 4p-3d Coulomb interactions. These include off-diagonal couplings between d states which may be important for singlet-triplet energy differences as well as providing pathways for symmetry-allowed dd excitations. We also neglect exchange interactions involving the 1s core-hole, which are very small.

In what follows, we use a standard set of parameters [in eV] [1]:  $t_{pd} = 1.1$ ;  $t_{pp} = 0.5$ ;  $t_{pp}^0 = 0.538$ ;  $t_{pd} = 0$ ;  $d_z = 1.7$ ;  $\epsilon_p = \epsilon_d = 3.5$ ;  $U_{pp} = 6$ ;  $U_{dd} = 8.8$ , and

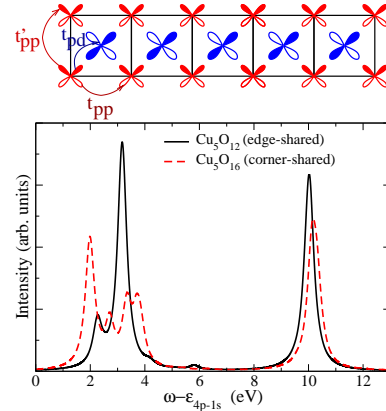


FIG. 1: Top: Edge-shared  $Cu_5O_{12}$  cluster. Bottom: XPS spectrum as a function of photon energy transfer and incident photon energy, for corner and edge-sharing copper-oxide clusters.

$U_Q = 8$ . These parameters give a value for the copper magnetic exchange  $J = 0.14$  eV for corner-shared copper oxides, and 2.8 meV for edge-shared.

We first perform exact-diagonalization of the Hamiltonian without the core-hole, and then redo the calculation with the core-hole. Since the Hamiltonian conserves the total spin, we diagonalized in the  $S = 1/2$  sector. From the eigenvalues and eigenvectors of the two steps, the RIXS spectrum is computed from Eq. (1).

In core level x-ray photoelectron spectroscopy (XPS), the final state corresponds to an intermediate state in the RIXS process. We first plot the XPS spectrum for both edge-shared cluster  $Cu_5O_{12}$  and corner-shared cluster  $Cu_5O_{16}$  in Fig. (1). In both cases, the prominent features correspond largely to 1) a non-locally screened d-inter-site ZRS ( $d^9L$ ) feature at 2.2 eV, where the core hole has pushed a  $d^9$  hole from the on-site Cu onto the oxygen ligands in the neighboring plaquette, 2) a local charge transfer (CT) excitation ( $d^{10}L$ ) at 3.5 eV whereby the screening of the core hole comes from the charge transfer from the copper to the oxygen ligand on the same plaquette, and 3) a 10 eV high-energy poorly screened  $d^9$  Cu hole on the core-hole site. These results are quantitatively similar to those presented earlier [14], apart from a more realistic value of the exchange  $J$  in the corner-shared geometry. We note that x-ray absorption spectra

in an extended system can be obtained from our XPS spectrum via a convolution with the copper 4p density of states, giving a broad absorption edge followed by spectral intensity extending higher in energy governed by the 4p bandwidth.

These excitations, present in both corner and edge-shared geometries, occur at roughly the same energy since they are governed by charge transfer energies and the exchange /  $t_{pd}^2$  between copper and oxygen: the Cu-Cu exchange does not play a major role in setting these energy scales.

The main difference concerns the prominence of the non-locally screened intersite d-ZRS excitation in the corner-shared compared with the edge-shared systems. While the ZRS accounts for nearly 80 percent of the ground state wavefunction including the core hole for the corner-shared plaquettes, it is approximately 56 % for the edge-shared system, reflecting the number of oxygen hybridization pathways available in the edge-shared configuration [15]. Thus while the energy is comparable in both systems, the matrix elements are much weaker at the ZRS scale in the edge-shared compared to corner-shared systems. In addition, the mobility of the ZRS for each geometry determines the peak widths, reflecting the splitting between bonding and anti-bonding ZRS on sites neighboring the core hole. In the case of the corner-shared systems, this corresponds to  $2t = 0.7\text{eV}$ , while due to the orientation of the orbitals in the edge-shared systems, the splitting is  $2t^0 = 0.3\text{eV}$ . As a result, the locally screened  $d^{10}L$  peak at 3.1 eV is much larger in edge-shared compared to corner-shared. This has led to the association of the phenomenon of high-temperature superconductivity occurring in corner-shared compounds and its absence in edge-shared compounds with the stability of the ZRS [16]. We note that the primary role of the oxygen orientation in the formation of the ZRS is not captured in single-band Hubbard model calculations.

We present the RIXS spectrum and resonant profile for a  $\text{Cu}_3\text{O}_8$  cluster in the inset of Fig. 2a. The parameters we have chosen are the same as for XPS in Fig. 1, appropriate for  $\text{Li}_2\text{CuO}_2$ . Here the intermediate state core-hole is included on the edge of the cluster, although our results do not qualitatively change if the core-hole is placed on the center plaquette. The RIXS spectrum consists of two prominent excitations at approximately  $\omega = 5.07\text{eV}$  energy transfer, at incident photon energies of 3.1 and 10 eV. This is the local CT excitation, resonant at both the locally screened  $d^{10}L$  CT and poorly screened  $d^9$  intermediate states, as shown in Fig. 1. In addition a weaker d-intersite ZRS-derived peak is present at  $\omega = 2.2\text{eV}$ , resonant for incident photon energies near 2.2 eV above the  $1s \rightarrow 4p$  transition. The XPS spectra can thus be viewed as a cut of the RIXS spectrum for a given incident photon energy  $\sim \omega_i$  summed over all Raman shifts.

In Fig. 2a we show a blow up of the low energy RIXS

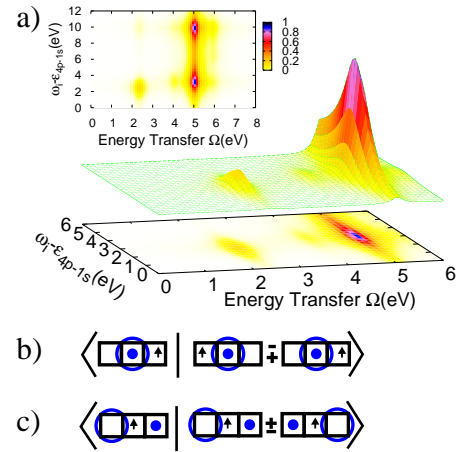


FIG. 2: a) RIXS spectra for  $\text{Cu}_3\text{O}_8$  cluster as a function of both photon energy transfer and incident photon energy  $\omega_i$ , measured relative to the binding energy  $E_{4p-1s}$ . The inset shows a contour map over large frequencies. Matrix elements for  $\text{Cu}_3\text{O}_8$  are shown in b) & c), for the main peaks in RIXS at  $(\omega_i - E_{4p-1s}; \Omega) = (2.2; 2.2)$  and  $(3.1; 5.07)$ , eV respectively. Here the left, right eigenvector is the core hole, final state, respectively, and the dot and the circle represent a singlet state formed by a hole on the copper site (dot) and a hole delocalized on the oxygens having the ZR symmetry (circle).

spectrum. Examining the symmetries of the core-hole and final state wavefunctions, the nature of the RIXS excitations, and the origin of their resonant profile, can be determined by inspection of matrix elements appearing in Eq. 1. The ground state without the core hole  $|j_0\rangle$  is largely of  $d^9$  character in each plaquette. Only those intermediate states which have a large overlap with the ground state are relevant to the RIXS process. To determine which final states  $|j_{\neq 0}\rangle$  are probed by RIXS and at what resonant energy they occur, one inspects the overlap of the core hole states  $|j_c\rangle$  reachable via the ground state without the core hole  $|j_0\rangle$ , with other excited states  $|j_{\neq 0}\rangle$  in the same Hilbert space. For example, since the ground state of the cluster  $|j_0\rangle$  is a singlet, it cannot be coupled to triplet intermediate states having a core hole. We immediately conclude that for our cluster all triplet states do not appear in the RIXS process without spin-orbit coupling.

We sketch schematically in Fig. 2b and 2c the leading order contributions to the wave functions of the intermediate state with the core-hole and the final state with large matrix overlap, which correspond to the main excitations shown in the RIXS spectra. While the intermediate state is predominantly one configuration, the final states can either be bonding or anti-bonding combinations of excitations on the plaquettes, at energies approximately 2 eV above  $E_0$ , split by ZRS hopping.

In Fig. 2b, it is clear that the resonance peak at  $\omega_i - E_{4p-1s} = 2.2\text{eV}$  and energy transfer  $\Omega = 2.2\text{eV}$  comes

from the combination of intermediate and final states corresponding to the creation of the ZRS in the final state, having strong overlap with the non-local, well-screened  $d^9L$  intermediate state. The two final states of bonding and antibonding combinations of ZRS on the two plaquettes couple to the intermediate state, with a weak splitting in edge-shared systems. Even with our broadening of 0.1 eV the separate peaks are difficult to resolve.

The final states of the higher energy peak correspond to bonding and antibonding combinations of  $d^{10}L$ , having strong overlap with the intermediate core hole state with the ligand on the core hole site as shown in Fig. 2c. This lies at higher energy  $\epsilon_{i-4p-1s} = 3.07$  eV, and is the most prominent final state in XPS shown in Fig. (1).

We note that we do not find prominent  $d-d$  excitations lying in the relevant energy range below 2 eV, even when including other  $d$  orbitals [17]. This follows from a symmetry analysis of the states, whereby  $d^9L$  and  $d^{10}L$  configurations cannot hybridize other Cu  $d$  orbitals and combinations of oxygen ligands. Thus direct  $d-d$  excitations are inaccessible in our model, in agreement with electron energy loss cluster calculations [18]. It is plausible that  $d-d$  excitations may arise if symmetry-breaking interactions with the 4p are included. This is different for oxygen 1s RIXS, as the creation of the core hole breaks this symmetry, allowing direct  $d-d$  excitations, as determined in recent cluster calculations [19].

The energy scale, prominence of the local CT excitation, and the double resonance profile shown in Figs. 1 and 2 correspond well to the RIXS data on  $\text{Li}_2\text{CuO}_2$  [8, 9]. While Ref. 8 attributed the weak 2.1 eV peak to an interatomic  $d-d$  excitation, and the strong peak at 5.4 eV peak to local CT excitation, in view of our results we would conclude that the low energy excitation rather corresponds to the intersite  $d$ -ZRS excitation. The weak peak observed at 7.6 eV however has no correspondance in our calculations. This peak may be associated with a local CT excitation into states with different ligand symmetry orthogonal to the ZRS ligand states, which may become accessible once oxygen 4p-2p interactions are included.

We now compare results for different edge-shared cuprates  $\text{Li}_2\text{CuO}_2$  and  $\text{CuGeO}_3$ . As pointed out in Ref. 6, the large valency of  $\text{Ge}^{4+}$  nearby the  $\text{CuO}$  planes increases the Madelung energy difference between the Cu and planar O sites in  $\text{CuGeO}_3$  compared to  $\text{LiCuO}_2$ , leading to the values  $\epsilon_{i-4p-1s} = 4.9$  and 3.2 eV, respectively, for each system. Since this energy scale largely determines the energies of the intersite ZRS and the separation in energy to the local CT excitation, the RIXS spectrum and resonance profile should be largely different in the two cases.

In Fig. (3) we present results for the RIXS spectrum for parameters corresponding to  $\text{CuGeO}_3$ , which are the same set of parameters as before apart from the change  $t_{pd} = 1.23$  eV, and  $\epsilon_{i-4p-1s} = 4.9$  eV. The larger value of

leads to several changes compared to the RIXS spectrum for  $\text{Li}_2\text{CuO}_2$  parameters. First, we note that the intersite ZRS peak has moved higher in energy from the  $d^9$  and core-hole ground states, lying at a photon energy transfer of 3.1 eV, and resonant at a higher incident photon energy  $\epsilon_{i-4p-1s} = 3.1$  eV. The bonding-antibonding splitting is smaller and the resonant peaks are more sharp. In addition, the CT ( $d^{10}L$ ) excitations move higher in energy, lying at  $\epsilon_{i-4p-1s} = 3.9$  eV and  $\epsilon_{i-4p-1s} = 6.2$  eV. This energy cost arises from the higher oxygen site energies as well as the reduction in exchange energy gain with the Cu spin.

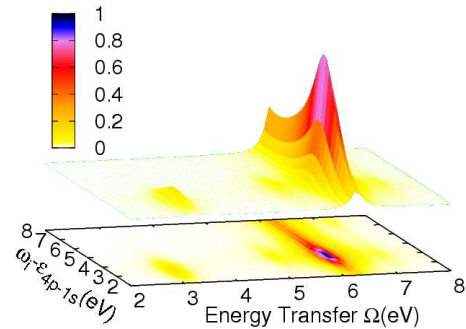


FIG. 3: RIXS spectra as a function of photon energy transfer and incident photon energy for parameters corresponding to  $\text{CuGeO}_3$ , as defined in the text.

All of these features both quantitatively and qualitatively reproduce the shape, energy, and width of the spectral features and resonance profile shown in  $\text{CuGeO}_3$  [9, 10, 11, 12], indicating that the local cluster model can adequately reproduce the data for photon energy losses in the energy range of 2-7 eV. We again remark that  $d-d$  excitations are not captured in the model, and further, that spin- $\uparrow\downarrow$  excitations, which require large clusters to observe bimagnon spin rearrangements at long wavelengths, are also very weak.

In summary, we have explored the Cu K edge spectrum for different edge-shared copper oxide systems, and have shown that the energy scales, peak intensities, and resonance profiles can be explained qualitatively within the context of exact diagonalization studies of the multi-band Hubbard model. The prospect of mapping out the full momentum, photon polarization, and resonance profile dependences would allow for a direct spectral check of the many roles played by local electronic correlations in the multi-band Hubbard approach. This remains a topic of future research.

[1] F. C. Zhang and T. M. Rice, Phys. Rev. B 37, 3759 (1988); H. Eskes et al., Phys. Rev. Lett. 61, 1415 (1988); Phys. Rev. B 41, 288 (1990); 44, 9656 (1991).

- [2] J. G. Rafet et al, cond-m at/0610313; cond-m at/0607319; T. Valla et al, cond-m at/0610249; B. P. Xie et al, cond-m at/0607450; W. Meevasana et al, cond-m at/0612541.
- [3] A. Damascelli, Z. Hussain, and Z.-X. Shen, *Rev. Mod. Phys.* **75**, 473 (2003).
- [4] T. P. Devereaux and R. Hackl, to appear in *Rev. Mod. Phys.* (2007).
- [5] P. M. Platzman and E. D. Isaacs, *Phys. Rev. B* **57**, 11107 (1998); A. Kotani and Shin, *Rev. Mod. Phys.* **73**, 203 (2001).
- [6] Y. Mizuno et al, *Phys. Rev. B* **57**, 5326 (1998).
- [7] J. B. Goodenough, *Phys. Rev.* **100**, 564 (1955); J. Kanamori, *J. Phys. Chem. Solids* **10**, 87 (1959); P. W. Anderson, *Solid State Phys.* **14**, 99 (1963).
- [8] Y.-K. Kim et al, *Phys. Rev. B* **69**, 155105 (2004).
- [9] D. Qian et al, *J. Phys. Chem. Solids* **66** 2212, (2005).
- [10] M. Z. Hasan et al, *Int. Journ. Mod. Phys. B* **17**, 3519 (2003).
- [11] S. Suga et al, *Phys. Rev. B* **72**, 081101 (2005).
- [12] M. v. Zimmermann et al, preprint.
- [13] L.-C. Duda et al, *Phys. Rev. B* **61**, 4186 (2000).
- [14] M. A. van Veenendaal et al, *Phys. Rev. B* **47**, 11462 (1993); **74**, 085118 (2006); K. Okada and A. Kotani, *J. Phys. Soc. Japan*, **75**, 044702 (2006).
- [15] Due to the one-dimension geometry of the clusters, especially for the corner-shared case, the  $d^3L$  is not truly a ZRS as it has more weight on the central bridging oxygen. However, the symmetry of this state remains ZR-like, maintaining the ZR signs of the ligands.
- [16] Y. Ohta et al, *Phys. Rev. B* **43**, 2968 (1991); C. Di Castro et al, *Phys. Rev. Lett.* **66**, 3209 (1991); J. H. Jefferson et al, *Phys. Rev. B* **45**, 7959 (1992); L. F. Feiner et al, *Phys. Rev. B* **45**, 10647 (1992); R. Raimondiet al, *Phys. Rev. B* **53**, 8774 (1996).
- [17] C. de Graaf and R. Broer, *Phys. Rev. B* **62**, 702 (2000).
- [18] S. Aitzkem et al, *Phys. Rev. B* **64**, 075112 (2001).
- [19] K. Okada and A. Kotani, *Phys. Rev. B* **63**, 045103 (2001).
- [20] The authors wish to thank Z.-X. Shen, Z. Hussain, M. Z. Hasan, M. G. Reven, M. G. Ingras, and J. Hancock for many useful discussions. TPD and GAS would like to acknowledge support of this work in part by NSERC, CFI, ONR Grant N00014-05-1-0127 (TPD), PREA (TPD), the Alexander von Humboldt Foundation (TPD) and CIAR (GAS). TPD wishes to thank the Pacific Institute for Theoretical Physics for their hospitality.